

## RESEARCH ARTICLE

# THE THERAPEUTIC EFFECTS OF MAGNETIC NANOPARTICLES HYPERTHERMIA ON LIVER CANCER : *IN VITRO* AND *IN VIVO* STUDIES

Hemely A. Hassan<sup>1</sup>; Khaled Ebnalwaled<sup>2,3</sup>; Huda Y. Gedawy<sup>1</sup>;  
Nadia S. Mahrous<sup>1\*</sup>

<sup>1</sup>Zoology Department, Faculty of Science, South Valley University, Qena, Egypt

<sup>2</sup>Electronics and Nano Devices Lab, Physics Department, Faculty of Science, South Valley University, Qena, Egypt

<sup>3</sup>Faculty of Nanotechnology for Postgraduate Studies, Cairo University, Sheikh Zayed Campus, Giza, Egypt

## ABSTRACT

Magnetic fluid hyperthermia is a modern cancer treatment that selectively heats tumor tissues to destroy them without harming healthy tissues. The current study aimed to evaluate the cytotoxic effect of Fe<sub>3</sub>O<sub>4</sub>/chitosan nanocomposite hyperthermia on liver cancer both *in vitro* and *in vivo*. The nanocomposite was prepared using the co-precipitation technique; and its magnetic and optical properties were measured along with its Raman spectrum. Cell toxicity for Fe<sub>3</sub>O<sub>4</sub>/chitosan nanocomposite was conducted on a liver cancer cell line (HepG2) using 3-(4,5-dimethylthiazol-2-yl) 2,5-diphenyltetrazolium bromide (MTT) assay, and the cell viability was performed after exposure to Fe<sub>3</sub>O<sub>4</sub>/chitosan nanocomposite hyperthermia using trypan blue stain. For the *in vivo* experiments, 25 male BALB/c albino mice were randomly/equally allotted into five groups: the 1<sup>st</sup> group was the non-tumor control group, the 2<sup>nd</sup> group involved the tumor-bearing control mice, the 3<sup>rd</sup> group involved the tumor-bearing mice received intramuscular injection of Fe<sub>3</sub>O<sub>4</sub>/chitosan (90 mg/kg, once/week for two weeks), the 4<sup>th</sup> and 5<sup>th</sup> groups involved tumor-bearing mice received intramuscular injection of Fe<sub>3</sub>O<sub>4</sub>/chitosan and exposed to an alternating magnetic field with a frequency of "200 kHz" and an output current of "300 A" once or twice/week, respectively, for two weeks. The results showed that nanocomposite was able to induce cytotoxicity (*in vitro*), as well as enhanced programmed cell death and necrosis of tumor cells, and reduced significantly ( $P < 0.05$ ) the tumor size (*in vivo*), when exposed to a hyperthermal magnetic field. In conclusion, Fe<sub>3</sub>O<sub>4</sub>/chitosan nanocomposite could be a promising therapeutic option for liver cancer through magnetic heating technology.

## Article History:

Received: 23 July 2023

Revised: 6 September 2023

Accepted: 22 September 2023

Published Online:

29 September 2023

## Keywords:

Apoptosis

Fe<sub>3</sub>O<sub>4</sub>/chitosan nanocomposite

HepG<sub>2</sub>

Magnetic hyperthermia

P53

## \*Correspondence:

Nadia Mahrous

Zoology Department

Faculty of Science

South Valley University,

Qena, Egypt

E-mail:

[samirnadia89@gmail.com](mailto:samirnadia89@gmail.com)

## INTRODUCTION

Hepatocellular carcinoma (HCC) is a type of cancer that arises from the liver and is recognized as the sixth most prevalent

cancer globally. Moreover, it is considered the third most common cause of cancer-related deaths across the world<sup>[1]</sup>. According to a study that estimated global cancer

incidence and mortality, liver cancer accounted for 19% of all newly diagnosed cancer cases across all ages and genders, with an incidence rate of 32% and a mortality rate of 31%<sup>[1]</sup>. Therefore, early detection and diagnosis of HCC are crucial for the effective treatment and improved survival of patients with HCC.

Magnetic fluid hyperthermia (MFH) is a novel and hopeful approach in the field of cancer treatment<sup>[2]</sup>. It involves the use of magnetic nanoparticles (MNPs) for hyperthermia therapy, which has the potential to be an effective modality for treating cancer. The fundamental concept of this technique is to target and harm cancer cells selectively by elevating their temperature through the use of MNPs, while minimizing the impact on normal tissues, thereby avoiding fatal effects<sup>[2]</sup>. Nanosystems can be designed to generate heat, making them suitable for use as hyperthermia agents that can deliver toxic amounts of thermal energy to tumors. Additionally, they can function as chemotherapy and radiotherapy enhancers, where a moderate degree of tissue warming can enhance the effectiveness of cell destruction<sup>[3]</sup>.

MNPs are typically composed of one or more inorganic crystals of a magnetic material that are either coated with or embedded within a biocompatible polymer, gold, or silica shell to enable functionalization. MNPs have a broad range of applications in the biomedical field due to their versatility. Iron oxides have gained significant attention in biomedical applications due to their unique ability to generate mechanical motion (linear or rotational, depending on the size and domain state of the particles) or dissipate thermal energy in response to external magnetic fields<sup>[3-5]</sup>. This property makes them highly advantageous for use in various medical applications. Iron oxides have demonstrated promising potential in this regard<sup>[3-5]</sup>. Fe<sub>3</sub>O<sub>4</sub>/chitosan nanocomposites have gained significant attention among magnetic materials due to their potential biomedical applications<sup>[6]</sup>. Fe<sub>3</sub>O<sub>4</sub> Nps are

easy to synthesize, biocompatible, non-toxic, chemically rather stable, and can be superparamagnetic. Surface coatings of Nps are an integral part of their synthesis<sup>[7]</sup>. Chitosan is a modified carbohydrate polymer that is derived from chitin, a natural biopolymer that is found in the shells of crabs, lobsters, yeast, and fungi<sup>[8]</sup>.

The focus of this study was to synthesize a thermally sensitive material called Fe<sub>3</sub>O<sub>4</sub>/chitosan nanocomposite and evaluate its therapeutic potential using an alternating magnetic field (AMF) on liver cancer cells, both *in vitro* and *in vivo*. The results of this study may provide valuable insights into the potential use of Fe<sub>3</sub>O<sub>4</sub>/chitosan nanocomposites for cancer treatment.

## MATERIAL AND METHODS

### Chemicals and kits

FeCl<sub>3</sub>.6H<sub>2</sub>O, Fe<sub>2</sub>SO<sub>4</sub>.7H<sub>2</sub>O, trypan blue stain, and low molecular weight chitosan molecules with a viscosity of 20 centipoise were obtained from Sigma-Aldrich (St. Louis, MO, USA). Dulbecco's modified Eagle's medium (DMEM), 3-(4,5-dimethylthiazol-2-yl) 2,5-diphenyltetrazolium bromide (MTT), penicillin, and streptomycin were purchased from PAA Laboratories GmbH (Pasching, Austria). The genomic DNA miniprep kit was obtained from QIAGEN (Hilden, Germany), and Lambda DNA/EcoRI + HindIII DNA ladder, GeneJET RNA purification kit, and Revert Aid™ First Strand cDNA synthesis kit were procured from ThermoFisher Scientific (Waltham, MA, United States). The Enzyme linked immunosorbent assay (ELISA) plate reader was obtained from BioTech Instruments (Winooski, VT, USA). The ELISA techniques were performed utilizing Novus Biologicals kits (Centennial, CO, USA). Other used laboratory chemicals were of pure quality and obtained from Sigma-Aldrich.

### Synthesis and characterization of Fe<sub>3</sub>O<sub>4</sub>/chitosan nanocomposite

Chitosan-coated Fe<sub>3</sub>O<sub>4</sub> Nps were synthesized using the coprecipitation technique.

Firstly, 0.02 mol of  $\text{FeCl}_3 \cdot 6\text{H}_2\text{O}$ , and 0.01 mol  $\text{Fe}_2\text{SO}_4 \cdot 7\text{H}_2\text{O}$  at a ratio of 2:1 was dissolved in 200 mL distilled water. To coat chitosan molecules onto the surface of superparamagnetic iron oxide Nps (SPIO-Nps), chitosan was adsorbed onto the Nps during their synthesis. An aqueous solution (1%, weight/volume) was prepared by adding 0.2 g of chitosan into a mixture of 19 mL of water and 1.0 mL of 2 mol acetic acid. The pH of the aqueous solution (200 mL) and the diluted chitosan was adjusted to 6.9 by slowly adding 20 mL of 30% (weight/weight) aqueous  $\text{NH}_4\text{OH}$ . This allowed for the successful coating of chitosan onto the surface of the SPIO-Nps, while stirring constantly under a temperature of  $80^\circ\text{C}$  for 20 minutes. The mixture's color turned from brown to black, followed by the standing of the solution for 24 hours. After the synthesis of  $\text{Fe}_3\text{O}_4$ /chitosan nanocomposite, a black precipitate was obtained. The precipitate was collected and washed multiple times. Finally, the  $\text{Fe}_3\text{O}_4$ /chitosan nanocomposite was dried at  $60^\circ\text{C}$  to obtain the final product. The drying process is essential to remove any residual solvent and ensure the stability of the nanocomposite material.

To assess the phase composition and crystallinity of nanocomposite, X-ray diffraction (XRD) was carried out employing a Bruker D8 X-ray diffractometer with monochromatized  $\text{Cu K}\alpha$  radiation. The Nps' morphology was investigated using high-resolution transmission electron microscopy (HRTEM) with a JEOL JEM-A 2100 instrument (Tokyo, Japan). Moreover, Fourier-transform infrared (FTIR) spectroscopy was utilized to examine the functional groups present in the prepared samples. The FTIR spectra of the  $\text{Fe}_3\text{O}_4$ /chitosan nanocomposite were captured utilizing a Jasco Model 4100 instrument (Tokyo, Japan), in the range of  $4000\text{-}400\text{ cm}^{-1}$ .

### Cell Culture

Liver cancer cell line (HepG2) utilized in the study was procured from the Research and Development Sector of The Holding

Company to produce Vaccines, Sera, and Drugs (VACSERA), situated in Cairo, Egypt. The cells were maintained in DMEM supplemented with 10% fetal bovine serum and 100 U/mL of both penicillin and streptomycin, and incubated in a humidified atmosphere containing 5%  $\text{CO}_2$  at  $37^\circ\text{C}$ . To maintain cell viability and ensure optimal growth conditions, the growth medium was replenished every 24 hours during the incubation period.

### MTT Assay

Before conducting the hyperthermia study, the synthesized  $\text{Fe}_3\text{O}_4$ /chitosan nanocomposite's cytotoxicity was assessed following the method detailed by Gerlier and Thomasset<sup>[9]</sup>. HepG2 cells were seeded in a 96-well plate at a density of  $5 \times 10^6$  cells per well and cultured in 100  $\mu\text{L}$  of DMEM. The culture medium was supplemented with varying concentrations of  $\text{Fe}_3\text{O}_4$ /chitosan nanocomposite (0, 15, 30, 60, 125, and 250  $\mu\text{g/mL}$ ), and the cells were then incubated at  $37^\circ\text{C}$  for 24 hours. Following incubation, 10  $\mu\text{L}$  of MTT reagent was added to each well, and the cells were further incubated for 2-4 hours at  $37^\circ\text{C}$ . Next, 200  $\mu\text{L}$  of dimethyl sulfoxide (DMSO) was added to each well and mixed thoroughly. To assess cell viability and determine any potential cytotoxic effects of the nanocomposite on the HepG2 cells, the absorbance was measured at 570 nm using a multi-well, BioTech, ELISA plate reader.

### $\text{Fe}_3\text{O}_4$ /chitosan nanocomposite hyperthermia assay

To investigate the *in vitro* hyperthermia effects of  $\text{Fe}_3\text{O}_4$ /chitosan nanocomposite, HepG2 cells were firstly cultured in a 6-well plate with 3 mL DMEM media for 24 hours at  $37^\circ\text{C}$ , and secondary cultured for 48 hours as follows:

- Control group: HepG2 culture medium only.
- Magnetic fluid (MF) group: various concentrations (15, 30, 60, 125, and 250  $\mu\text{g}$ ) of  $\text{Fe}_3\text{O}_4$ /chitosan nanocomposite per mL HepG2 culture medium.

- MFH group: various concentrations (15, 30, 60, 125, and 250  $\mu\text{g}$ ) of  $\text{Fe}_3\text{O}_4$ /chitosan nanocomposite per mL HepG<sub>2</sub> culture medium and heated by AMF.

To achieve MFH, the  $\text{Fe}_3\text{O}_4$ /chitosan nanocomposite sample was placed on the coil plate of a high-frequency heater and exposed to AMF with a frequency of 200 kHz and a power output of 4 kW for 15 minutes. The temperature of the sample was monitored and recorded using an infrared (IR) thermal camera to evaluate the heating efficiency and effectiveness of the MFH treatment. The cell viability was assessed by trypan blue staining.

#### Determination the median lethal dose (LD<sub>50</sub>) of $\text{Fe}_3\text{O}_4$ /chitosan nanocomposite in male BALB/c mice

Male BALB/c mice (8 animals/group) were intramuscularly injected with different doses of  $\text{Fe}_3\text{O}_4$ /chitosan nanocomposite (50, 100, 300, 500, and 700 mg/kg) and the mortality of the mice was recorded after 24 hours. The LD<sub>50</sub> of the  $\text{Fe}_3\text{O}_4$ /chitosan nanocomposite was determined by the following equation<sup>[10]</sup>:  $\text{LD}_{50} = \text{Dm} - \Sigma(\text{Z} \times \text{d}) / \text{n}$ ; where: (Dm) represents the minimum dose that kills all animals in the group, ( $\Sigma$ ) is the sum of ( $\text{Z} \times \text{d}$ ), (Z) is the mean number of dead animals in two successive groups, (d) is the constant factor between two successive groups, and (n) is the number of animals in each group (Table 1).

#### *In vivo* experiments

The study involved the use of 25 adult male BALB/c albino mice that were 10 weeks old and weighed between 25-30g. The mice used in the study were procured from the animal house of the Egyptian Organization for Biological Products and Vaccines, situated in Helwan, Cairo, Egypt. The mice were housed individually in plastic cages in a suitable condition, with a temperature range of 23-25°C and at 20±5% relative humidity, and were fed on balanced pellets with water free access. The mice were housed for two weeks before the experiment for accommodation in the surrounding environment.

To establish the tumor model, BALB/c mice were intramuscular injected in the femur with 0.1 mL cell suspension containing  $5 \times 10^6$  HepG<sub>2</sub> cells. The tumor were allowed to grow for a period of  $\geq 14$  days until it reached a diameter of approximately 300  $\text{mm}^3$ <sup>[11]</sup>. Tumor diameters are measured with calipers, and the tumor volume in  $\text{mm}^3$  is calculated by the following formula<sup>[11]</sup>:  $\text{Volume} = (\text{Width})^2 \times \text{Length} / 2$

The tumor-bearing mice were randomly allotted into four groups (5 mice for each group) as follows:

- The tumor control group involved the tumor-bearing mice that were intramuscularly injected with saline (NaCl 0.9%).

**Table 1:** Calculation of the median lethal dose (LD<sub>50</sub>) of  $\text{Fe}_3\text{O}_4$ /chitosan nanocomposite.

Dose of nanocomposite (mg/kg)	n	Number of dead animals	Z	d	(Z × d)
50	8	0	0	50	0
100	8	0	0	100	0
300	8	0	0	200	0
500	8	4	4	200	800
700	8	8	4	200	800

Z: is the mean number of dead animals in two successive groups; d: is the constant factor between two successive groups; n: is the number of animals in each group. LD<sub>50</sub> of  $\text{Fe}_3\text{O}_4$ /chitosan nanocomposite = 500 mg/kg.

- The MF group involved the tumor-bearing mice that were intramuscularly injected with 90 mg/kg of Fe<sub>3</sub>O<sub>4</sub>/chitosan nanocomposite (resembles 18% of LD<sub>50</sub>) once a week for two consecutive weeks.
- The MFH<sub>1</sub> group involved the tumor-bearing mice that were intramuscularly injected with 90 mg/kg of Fe<sub>3</sub>O<sub>4</sub>/chitosan nanocomposite and subjected to AMF with a frequency of 200 kHz, an output current of 300 A, and a power output of 4 kW<sup>[12]</sup> for 30 minutes once a week for 2 consecutive weeks. During the treatment, the temperature of the sample was continuously monitored and recorded using an IR thermal camera.
- The MFH<sub>2</sub> group involved the tumor-bearing mice that were intramuscularly injected with 90 mg/kg of Fe<sub>3</sub>O<sub>4</sub>/chitosan nanocomposite and subjected to AMF with a frequency of 200 kHz, an output current of 300 A, and a power output of 4 kW for 30 minutes twice a week for 2 consecutive weeks. During the treatment, the temperature of the sample was continuously monitored and recorded using an IR thermal camera.

In addition to above groups, another group containing 5 mice (without tumors) were injected intramuscularly with normal saline solution and considered as a non-tumor control group.

#### DNA fragmentation analysis

The tumors were utilized to extract DNA following the protocol recommended by the manufacturer for the GenElute Mammalian Genomic DNA Miniprep Kit (QIAGEN). Subsequently, 20 µL aliquots of the isolated DNA samples were loaded onto a 1% agarose gel containing 5 µg/mL ethidium bromide in 1× Tris-acetate-ethylene diamine tetra-acetic acid buffer (pH = 8.5). The gel was then subjected to electrophoresis at 90 V for 1.5 hours, and the DNA bands were visualized under ultraviolet (UV) light and compared with a DNA ladder (ThermoFisher Scientific) for analysis.

#### Reverse-transcriptase polymerase chain reaction (RT-PCR)

To assess the levels of expression of apoptosis-related genes in the tumor tissues, total RNA was extracted using the GeneJET RNA Purification kit (ThermoFisher Scientific), following the instructions provided by the manufacturer. The cDNA products from the high-quality RNA were carried out using Revert Aid™ First Strand cDNA synthesis kit (ThermoFisher Scientific) based on the manufacturer's protocols. The reaction mixture was performed in thermal cycler (Bio-Rad, Hercules, CA, USA) according to the manufacture protocol. Subsequently, a quantitative real-time PCR was conducted utilizing a combination of 12.5 µL of 2× SYBR green PCR master mix (ThermoFisher Scientific), 1.0 µL of each primer, 2 µL of cDNA, and 8.5 µL of RNase-free water; resulting in a total volume of 25 µL. The amplification conditions and cycle counts were set at an initial activation of 95°C for 15 min, followed by 40 cycles consisting of a denaturation step at 94°C for 15 seconds, followed by an annealing step at 60°C for 30 seconds, and an elongation step at 72°C for 30 seconds. The expression levels of the *P53*, *Casp3*, and *Bcl-2* genes were determined using the housekeeping gene *β-actin* as an internal control.

The first pair of primers is for the target gene *P53*, with the forward primer sequence being 5'-CCCCTCCTGGCCCCTGTCATCTTC-3' and the reverse primer sequence being 5'-GCAGCGCCTCACAACCTCCGTCAT-3'. The second pair of primers is for the target gene *Casp3*, with the forward primer being 5'-TTCATTATTTCAGGCC TGCCGAGG-3' and the reverse primer being 5'-TTCTGACAGGCCATGTCATCC TCA-3'. The third pair of primers is for the target gene *Bcl-2*, the forward primer sequence being 5'CCTGTGGATGACTGA GTACC-3' and the reverse primer being 5'-GAGACAGCC AGGAGAAATCA-3'. The fourth pair of primers is for the target gene *β-actin*, with the forward primer being

5'-CAAGGTCATCCATGACAACCTTTG-3', the reverse primer being 5' GTCCACCACCTGTTGCTGTAG-3'. All used primers in the current study were purchased from ThermoFisher Scientific.

#### Enzyme linked immunosorbent assay (ELISA)

To measure the serum concentrations of P53, BCL-2, and cleaved CASP3 proteins, a sandwich ELISA assay was performed using Novus Biologicals ELISA kits (Catalogue numbers: NBP2-75358, NBP2-69946, and DYC835-2, respectively) specific for mouse proteins following the manufacturer's protocol.

#### Statistical analysis

The statistical analysis was performed utilizing the SPSS program (IBM SPSS Inc., Chicago, IL, USA) and one-way analysis of variance. The least significant difference (LSD) was employed to assess the distinction between the treated groups;  $P$ -values  $< 0.05$  are considered significant.

## RESULTS

### Characterization of Fe<sub>3</sub>O<sub>4</sub>/chitosan nanocomposite

The XRD pattern displays six principal peaks at  $2\theta$  values of 30.3°, 36.5°, 44.0°, 54.0°, 57.0°, and 63.0°, which correspond to reflections from the 220, 311, 410, 422, 510, and 440 crystal planes, respectively (Figure 1). The positions and intensities of all peaks align with the cubic crystalline system of Fe<sub>3</sub>O<sub>4</sub> Nps. The results indicate that the Nps are pure Fe<sub>3</sub>O<sub>4</sub> with a cubic structure after surface modification (Figure 1). By utilizing the Scherer equation, the average size of the crystallites in the Nps was determined by correlating it with the broadening of the XRD peaks. The computed average crystallite size was 43 nm. High-resolution transmission electron microscopy (HR-TEM) was utilized to investigate the morphology of the Fe<sub>3</sub>O<sub>4</sub>/chitosan nano-composite and the resulting image is shown in Figure "2". Based on the image obtained from HR-TEM analysis, it can be observed that the MNps exhibit a spherical shape, and size was found to be in the range of 13-17 nm.

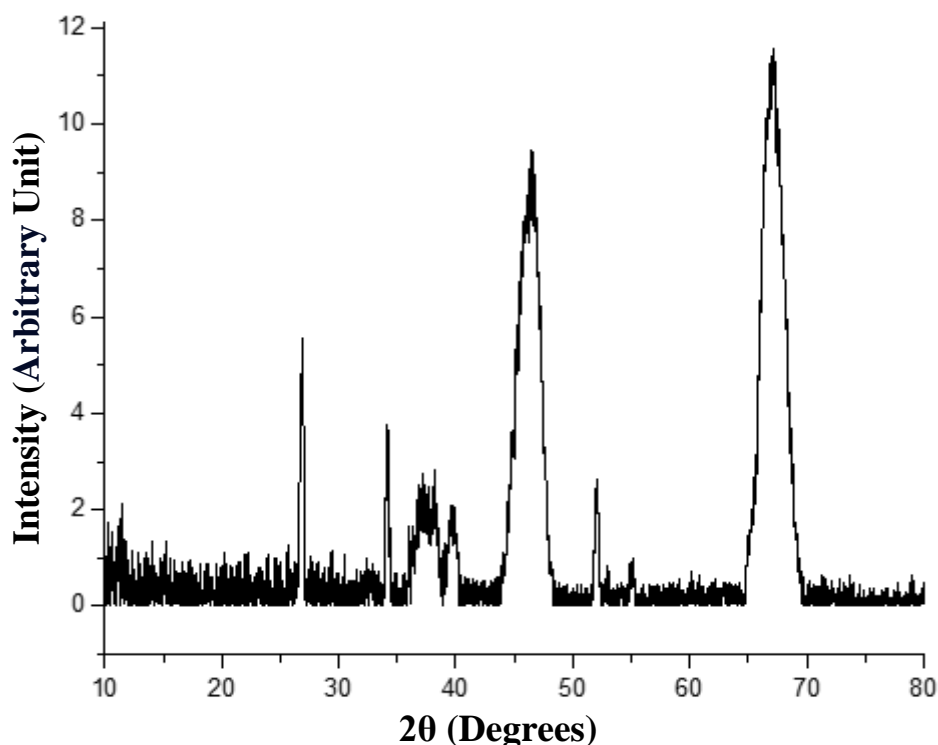


**Figure 1:** The X-ray diffraction spectra of Fe<sub>3</sub>O<sub>4</sub>/chitosan nanocomposite.

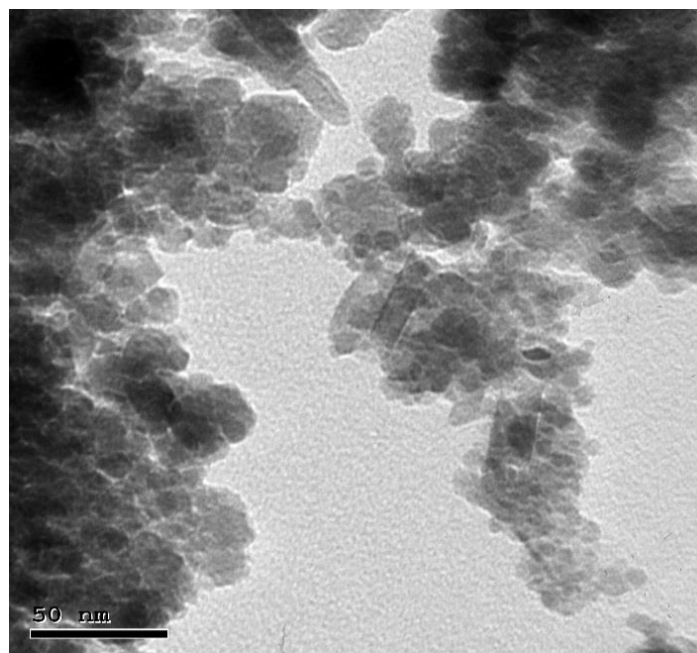


**Figure 2:** High-resolution transmission electron microscopy of  $\text{Fe}_3\text{O}_4$ /chitosan nanocomposite.

The spectrum of the  $\text{Fe}_3\text{O}_4$ /chitosan nanocomposite was obtained using FTIR analysis across a range of  $4000\text{--}400\text{ cm}^{-1}$ , as depicted in (Figure 3). The objective of the FTIR analysis was to verify the existence of functional groups on the surface of the synthesized nanocomposite material. The FTIR spectrum likely showed the characteristic peaks of both  $\text{Fe}_3\text{O}_4$  and chitosan. The emergence of a peak at  $2922\text{ cm}^{-1}$ , corresponding to the stretching

vibrations of  $\text{--CH--}$  in chitosan, is indicative of the presence of chitosan. Furthermore, the peak at  $1641\text{ cm}^{-1}$  can be attributed to the  $\text{N--H}$  vibration of chitosan, while the  $\text{C--N}$  vibration of the amino group is represented by the peak at  $1415\text{ cm}^{-1}$  and the  $\text{C--O}$  in the ether group is indicated by the peak at  $1074\text{ cm}^{-1}$ . These peaks confirm the presence of chitosan on the surface of the  $\text{Fe}_3\text{O}_4$  nanoparticles.

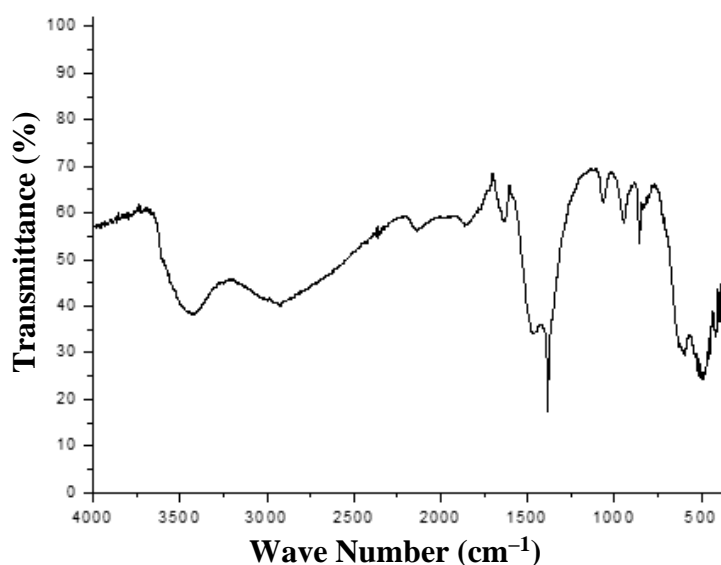


**Figure 3:** Fourier-transform infrared spectra of  $\text{Fe}_3\text{O}_4$ /chitosan nanocomposite.

### ***In vitro* cytotoxic effect of synthesized Fe<sub>3</sub>O<sub>4</sub>/chitosan nanocomposite with or without hyperthermia on HepG2 cells**

The cytotoxicity of the Fe<sub>3</sub>O<sub>4</sub>/chitosan nanocomposite at various concentrations with/without hyperthermia was *in vitro* evaluated against HepG<sub>2</sub> cells using the trypan blue staining and MTT assay, respectively (Figure 4). The data indicated a dose-dependent cytotoxic effect of the nanocomposite with/without hyperthermia, with the highest cell viability of 100% observed in the control group. The highest toxic effect of Fe<sub>3</sub>O<sub>4</sub>/chitosan nanocomposite in the absence of hyperthermia was

observed at a concentration of 250 µg/mL, where only 46.84% cell viability was observed after 24 hours of exposure. The highest toxic effect of Fe<sub>3</sub>O<sub>4</sub>/chitosan nanocomposite in the presence of hyperthermia (45-47°C for 15 minutes) was observed at a concentration of 250 µg/mL, where only 10.7% cell viability was observed after 48 hours of exposure (Figure 4). These results suggest that the Fe<sub>3</sub>O<sub>4</sub>/chitosan nanocomposite has a cytotoxic effect on HepG<sub>2</sub> cells, and the degree of cytotoxicity is dependent on the concentration, exposure time, and the absence/presence of hyperthermia.

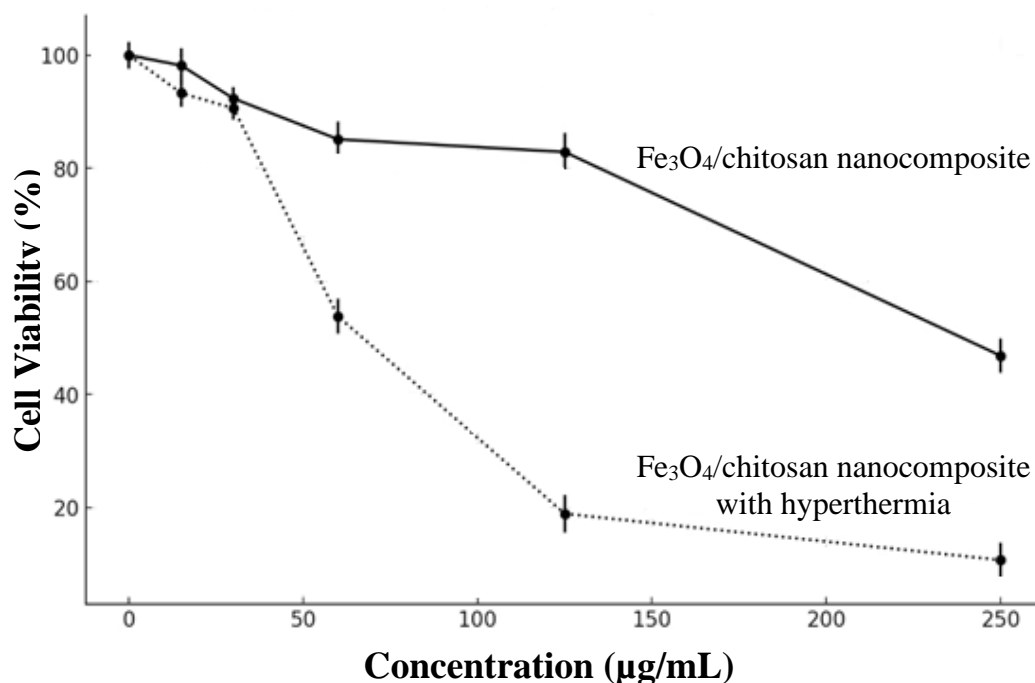


**Figure 4:** *In vitro* cytotoxic effect of synthesized Fe<sub>3</sub>O<sub>4</sub>/chitosan nanocomposite with/without hyperthermia on HepG<sub>2</sub> cells. The cell viability was assessed by trypan blue stain and MTT assay for Fe<sub>3</sub>O<sub>4</sub>/chitosan nanocomposite with/without hyperthermia, respectively. Data were presented as mean ± standard error. MTT: 3-(4,5-dimethylthiazol-2-yl) 2,5-diphenyltetrazolium bromide.

### ***In vivo* effect of synthesized Fe<sub>3</sub>O<sub>4</sub>/chitosan nanocomposite with or without hyperthermia on tumor volume, DNA fragmentation, and apoptotic markers**

The mice treated with Fe<sub>3</sub>O<sub>4</sub>/chitosan nanocomposite with AMF (200 kHz, 4 kW, output current 300 A) once per week for 2 weeks (MFH<sub>1</sub> group) showed a significant reduction in tumor growth (330.0±6.7 mm<sup>3</sup>)

compared with the tumor control mice (805.7±0.9 mm<sup>3</sup>) and MF (757.3±6.2 mm<sup>3</sup>) groups. However, the mice treated with Fe<sub>3</sub>O<sub>4</sub>/chitosan nanocomposite with AMF twice per week for 2 weeks (MFH<sub>2</sub> group) showed a significant reduction in tumor growth (185.1±4.9 mm<sup>3</sup>) compared with the MFH<sub>1</sub> mice (Figure 5).



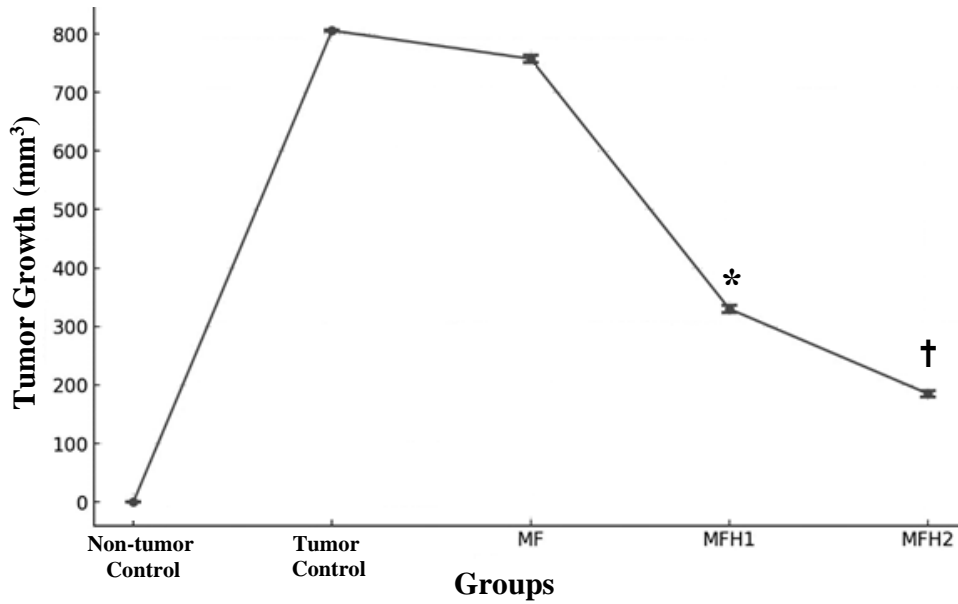


**Figure 5:** Effect of magnetic Fe<sub>3</sub>O<sub>4</sub>/chitosan nanocomposite on tumor volume. Data were presented as mean  $\pm$  standard error. MF: magnetic fluid; MFH: magnetic fluid hyperthermia; \*:  $P < 0.05$  compared with the tumor control and MF groups; †:  $P < 0.05$  compared with the MFH<sub>1</sub> group.

The MFH<sub>2</sub> group showed a higher degree of DNA fragmentation (which appears as a smear indicating necrosis) than the other groups (Figure 6). The expression of the proapoptotic genes (*P53* and *Casp3*) showed a significant increase in the MFH<sub>1</sub> ( $3.15 \pm 0.01$  and  $3.90 \pm 0.17$ ) and MFH<sub>2</sub> groups ( $5.05 \pm 0.15$  and  $5.49 \pm 0.13$ ), respectively, compared with the tumor control group ( $0.73 \pm 0.02$  and  $0.08 \pm 0.06$ , respectively) and

the MF group ( $2.03 \pm 0.03$  and  $2.25 \pm 0.07$ , respectively). In addition, the expression of the antiapoptotic gene *Bcl-2* showed a significant decrease after hyperthermia in the MFH<sub>1</sub> and MFH<sub>2</sub> groups ( $0.58 \pm 0.10$  and  $0.38 \pm 0.25$ , respectively) compared with the tumor control and MF groups ( $1.43 \pm 0.03$  and  $0.76 \pm 0.04$ , respectively) as shown in Figure "7".

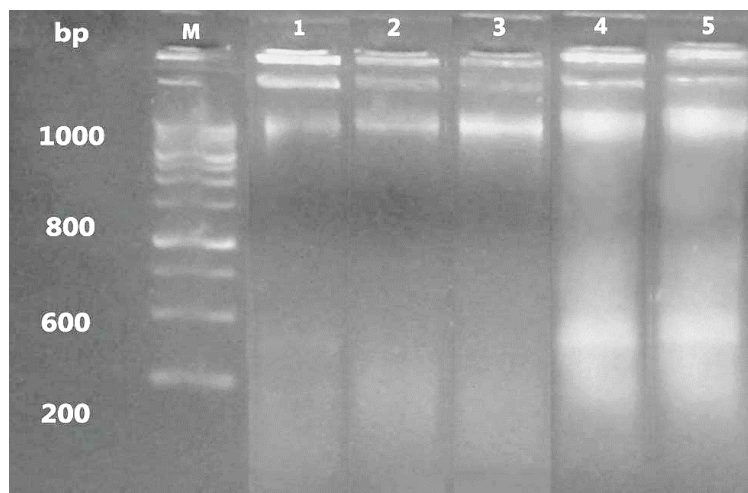


**Figure 6:** Effect of alternating magnetic field-induced Fe<sub>3</sub>O<sub>4</sub>/chitosan nanocomposite-mediated hyperthermia treatment on DNA fragmentation. (M) Ladder (200-1000 base pairs), (1) non-tumor control group, (2) tumor control group, (3) MF group, (4) MFH<sub>1</sub> group, (5) MFH<sub>2</sub> groups. MF: magnetic fluid; MFH: magnetic fluid hyperthermia.

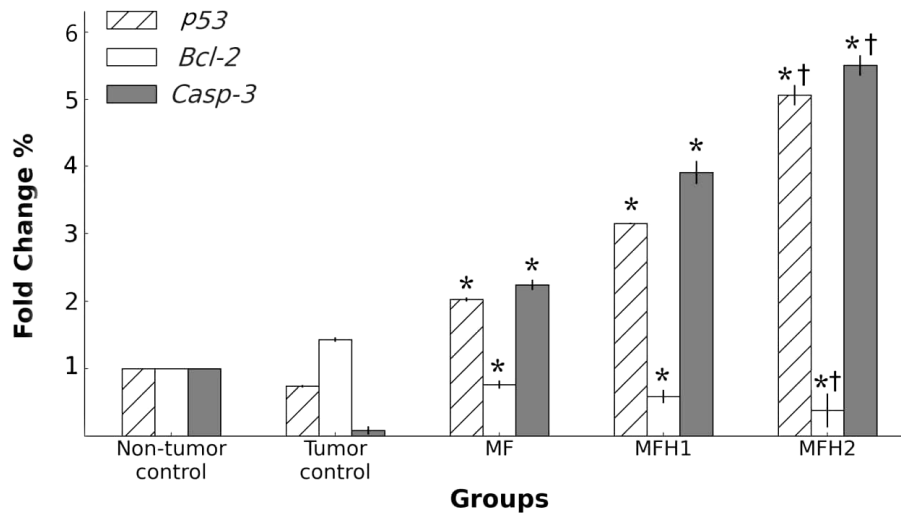


**Figure 7:** Effect of alternating magnetic field-induced  $\text{Fe}_3\text{O}_4$ /chitosan nanocomposite-mediated hyperthermia treatment on apoptosis-related genes' expression measured by RT-PCR. Data were presented as mean  $\pm$  standard error. MF: magnetic fluid; MFH: magnetic fluid hyperthermia; \*:  $P < 0.05$  compared with the tumor control group; †:  $P < 0.05$  compared with the MFH<sub>1</sub> group.

The concentrations of proapoptotic proteins, P53, and active CASP3 showed a significant increase in MFH<sub>1</sub> group ( $2.34 \pm 0.02$  and  $2.45 \pm 0.02$ ) and MFH<sub>2</sub> group ( $2.61 \pm 0.01$  and  $3.15 \pm 0.02$ ) compared with the tumor control group ( $0.39 \pm 0.02$  and  $0.65 \pm 0.03$ ) and MF group ( $1.44 \pm 0.01$  and  $2.07 \pm 0.12$ , respectively). Conversely, there

was a significant decrease in the concentration of the anti-apoptotic protein, BCL-2, after hyperthermia in MFH<sub>1</sub> and MFH<sub>2</sub> groups ( $0.84 \pm 0.02$  and  $0.62 \pm 0.04$ , respectively), compared with the control group and MF group ( $1.25 \pm 0.03$  and  $1.09 \pm 0.029$ , respectively) as shown in Figure "8".

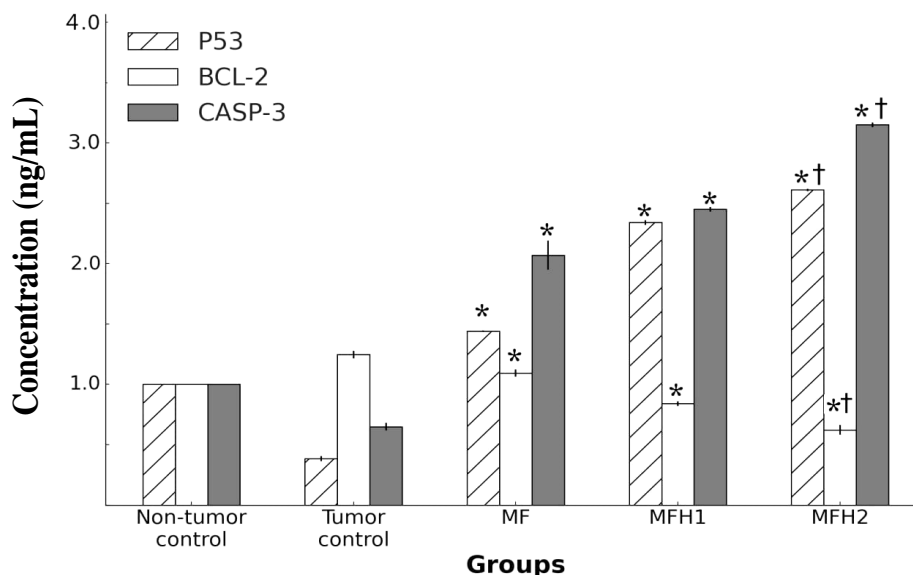


**Figure 8:** Effect of alternating magnetic field-induced  $\text{Fe}_3\text{O}_4$ /chitosan nanocomposite-mediated hyperthermia treatment on apoptosis-related protein concentrations measured by ELISA. Data were presented as mean  $\pm$  standard error. MF: magnetic fluid; MFH: magnetic fluid hyperthermia; \*:  $P < 0.05$  compared with the tumor control group; †:  $P < 0.05$  compared with the MFH<sub>1</sub> group.

## DISCUSSION

The results of FTIR analysis in this study are consistent with previous studies<sup>[13,14]</sup>, which confirmed the reliability and effectiveness of FTIR analysis for identifying the functional groups in the Fe<sub>3</sub>O<sub>4</sub>/chitosan nanocomposite. The presence of chitosan on the surface of Fe<sub>3</sub>O<sub>4</sub> Nps is significant because chitosan is a natural polymer with excellent biocompatibility and biodegradability, making it a promising material for various biomedical applications, and prevents agglomeration, oxidation, corrosion, and toxicity<sup>[15]</sup>. FTIR analysis provided information on the chemical composition and properties of the nanocomposite material, specifically the highly organized and oriented polymer chains of chitosan on the surface of Fe<sub>3</sub>O<sub>4</sub> Nps that were indicated by the stretching vibrations of –CH– and N–H. The stability and functionality of the nanocomposite material may be due to the presence of ether and amino groups, as indicated by the C–N and C–O vibration peaks.

The MTT assay used in this study is reliable for evaluating the cytotoxicity of the Fe<sub>3</sub>O<sub>4</sub>/chitosan nanocomposite on HepG2 cells. Bae *et al.*<sup>[16]</sup> reported that chitosan MNps did not exhibit serious toxicity to healthy tissue. However, other studies, such as that of Hosseinzadeh *et al.*<sup>[17]</sup>, have shown that chitosan can inhibit cell viability in a dose-dependent manner and induce apoptosis in colon cancer cell line "HT-29. Yan *et al.*<sup>[12]</sup> found that a large amount of Fe<sub>2</sub>O<sub>3</sub> Nps caused a high rate of apoptosis in the liver cancer cell line "SMMC-7721". Kowalik *et al.*<sup>[18]</sup> observed that Fe<sub>3</sub>O<sub>4</sub> Nps alone did not significantly impact the viability of breast cancer "4T1" cells, but reduced cancer cell viability in the presence of AMF. The present study's findings are consistent with previous researches, which have shown that hyperthermia treatment with MNp fluid (Fe<sub>3</sub>O<sub>4</sub>) can significantly decrease prostatic<sup>[19]</sup> and pancreatic<sup>[20]</sup> tumor growth. Qi *et al.*<sup>[21]</sup> demonstrated that chitosan Nps may have potential as an anti-

cancer agent for human hepatoma BEL7402 cells by decreasing cell proliferation through inducing cell necrosis. All of these findings suggest the potential of Fe<sub>3</sub>O<sub>4</sub>/chitosan nanocomposite for cancer therapy.

The observed reduction in tumor size following hyperthermia treatment may be attributed to several factors<sup>[22]</sup>. The cancerous tissue is believed to be more sensitive to heat than normal tissue due to the acidic and hypoxic conditions present within tumors<sup>[23]</sup>. Hypoxic cells in solid tumors are often more acidic and nutrient-deprived, making them more susceptible to thermal damage. Additionally, heat exposure can improve the local blood and oxygen supply to the tumor, facilitating drug penetration and inducing tumor cell death<sup>[24]</sup>. Hyperthermia treatment may also decrease DNA synthesis and stimulate lipid peroxidation, which can damage the cell membrane structure and lead to tumor cell death. According to Lin *et al.*<sup>[22]</sup>, hyperthermia treatment may hold potential as a cancer therapy, particularly when used in combination with other treatments such as drug delivery.

Kuppusamy and Karuppaiah<sup>[25]</sup> reported that chitosan Nps induced DNA fragmentation in T24 urinary bladder cancer cell lines. However, to our knowledge, no study has been conducted to investigate the impact of AMF-induced hyperthermia treatment using Fe<sub>3</sub>O<sub>4</sub>/chitosan nanocomposite on DNA fragmentation. This suggests a potential avenue for future research to explore the mechanisms underlying the cytotoxic effects of the nanocomposite under hyperthermia conditions. The modulation of pro- and anti-apoptotic genes (including *P53*, *Casp3*, and *Bcl-2*) may contribute to the mechanism underlying the cytotoxic effects of MFH treatment on cancer cells. The current study found that the expression of the pro-apoptotic genes (*P53* and *Casp3*) increased significantly in MFH<sub>1</sub> and MFH<sub>2</sub> treated groups compared with the tumor control and MF groups. The significant increase in the expression of these genes suggests that

MFH treatment can trigger programmed cell death in cancer cells. In addition, there was a significant decrease in the expression of the anti-apoptotic gene *Bcl-2* after hyperthermia in the MFH<sub>1</sub> and MFH<sub>2</sub> groups, compared with the tumor control and MF groups; this significant decrease in *Bcl-2* expression further supports the pro-apoptotic effects of MFH treatment. Overall, these findings suggested that MFH treatment has the potential to induce apoptosis in cancer cells by regulating the expression of pro- and anti-apoptotic genes. In addition, the current study observed an increase in the concentration of pro-apoptotic proteins "P53 and active CASP3" in the MFH<sub>1</sub> and MFH<sub>2</sub> groups compared with the tumor control and MF groups, indicating that MFH treatment may direct cancer cells toward apoptosis. Additionally, there was a significant decrease in the concentration of the anti-apoptotic protein BCL-2 after hyperthermia in the MFH<sub>1</sub> and MFH<sub>2</sub> groups, which further supported the pro-apoptotic effects of MFH treatment. Other studies indicated the effect of hyperthermia on apoptosis and proliferation of cancer cells<sup>[14,26,27]</sup>. Zavareh *et al.*<sup>[28]</sup> used MNPs containing fluorouracil (5-FU) to improve the chemotherapeutic effect in various cancer models. These investigations have demonstrated that the inclusion of 5-FU in MNPs can enhance the efficacy of chemotherapy treatment by reducing the expression of human Bcl-2 protein and elevating the expression of human Casp3 protein. Likewise, Jordan *et al.*<sup>[29]</sup> investigated the impact of MFH on C3H mammary carcinoma *in vivo* and observed widespread tumor necrosis after undergoing MFH treatment. In addition, Salimi *et al.*<sup>[30]</sup> investigated the use of dendrimer functionalized iron-oxide Nps in combination with MFH for the therapy of BALB/c mice with breast cancer. Based on the histopathological analysis, a significant augmentation in the number of apoptotic cells in the MNPs+AMF group was observed, in addition to a decrease in the micro-vessel density within the tumor, which could be another contributing factor

to the observed reduction in tumor size in the treated mice<sup>[30]</sup>.

Overall, the current study provided further evidence for the potential of MFH treatment and MNPs in cancer therapy. The use of MNPs in cancer therapy provides several benefits, such as targeted delivery and hyperthermia treatment. The MNPs can be modified with targeting agents, like antibodies or peptides, to specifically target cancer cells while minimizing damage to healthy tissue. These Nps can also be activated by an external magnetic field to generate heat and trigger cancer cell death. Combining MNPs with other cancer treatments, such as chemotherapy and radiation therapy, may enhance the effectiveness of cancer therapy while reducing the associated side effects. Further research is needed to optimize the use of MNPs in cancer therapy and to gain a better understanding of their mechanisms of action.

#### ETHICAL APPROVAL

The study was conducted following the guidelines set by the Ethical Committee of the Faculty of Science at South Valley University in Qena, Egypt, and was approved under the number 009/11/22.

#### FUNDING SOURCE DISCLOSURE

This manuscript received no funding.

#### CONFLICT OF INTEREST

The authors declare no conflict of interest.

#### REFERENCES

- [1] Ferlay, J.; Colombet, M.; Soerjomataram, I. *et al.* (2019). Estimating the global cancer incidence and mortality in 2018: GLOBOCAN sources and methods. *Int J cancer*, 144(8): 1941-1953.
- [2] Doaga, A.; Cojocariu, A. M.; Amin, W. *et al.* (2013). Synthesis and characterizations of manganese ferrites for hyperthermia applications. *Mater Chem Phys*, 143: 305-310.
- [3] Pankhurst, Q. A.; Connolly, J.; Jones, S. K. *et al.* (2003). Applications of magnetic nanoparticles in biomedicine.

- J Phys D Appl Phys, 36(13): R167 (DOI: 10.1088/0022-3727/36/13/201).
- [4] Kozissnik, B.; Bohorquez, A. C.; Dobson, J. *et al.* (2013). Magnetic fluid hyperthermia: advances, challenges, and opportunity. *Int J Hyperthermia*, 29(8): 706-714.
- [5] Pankhurst, Q. A.; Thanh, N. T. K.; Jones, S. K. *et al.* (2009). Progress in applications of magnetic nanoparticles in biomedicine. *J Phys D Appl Phys*, 42(22): 224001 (DOI: 10.1088/0022-3727/42/22/224001).
- [6] Thuy, T. T.; Maenosono, S. and Thanh, N. T. K. (2012). Next Generation Magnetic Nanoparticles for Biomedical Applications. In: *Magnetic Nanoparticles: From Fabrication to Clinical Applications* (Thanh, N. T. K., ed), pp: 98-128. CRC Press, New York, NY, USA.
- [7] Shubayev, V. I.; Pisanic II, T. R. and Jin, S. (2009). Magnetic nanoparticles for theragnostics. *Adv Drug Deliv Rev*, 61(6): 467-477.
- [8] Illum, L.; Jabbal-Gill, I.; Hinchcliffe, M. *et al.* (2001). Chitosan as a novel nasal delivery system for vaccines. *Adv Drug Deliv Rev*, 51(1-3): 81-96.
- [9] Gerlier, D. and Thomasset, N. (1986). Use of MTT colorimetric assay to measure cell activation. *J Immunol Methods*, 94(1-2): 57-63.
- [10] Wilbrandt, W. (1952). Behrens methods for calculation of LD<sub>50</sub>. *Arzneimittelforschung*, 2(11): 501-503.
- [11] Jin, Z.; Jia, B.-X.; Tan, L.-D. *et al.* (2020). Combination therapy with metformin and IL-12 to inhibit the growth of hepatic carcinoma by promoting apoptosis and autophagy in HepG2-bearing mice. *Eur Rev Med Pharmacol Sci*, 24(23): 12368-12379.
- [12] Yan, S. Y.; Chen, M. M.; Fan, J. G. *et al.* (2014). Therapeutic mechanism of treating SMMC-7721 liver cancer cells with magnetic fluid hyperthermia using Fe<sub>2</sub>O<sub>3</sub> nanoparticles. *Braz J Med Biol Res*, 47(11): 947-959.
- [13] Mondal, S.; Manivasagan, P.; Bharathiraja, S. *et al.* (2017). Hydroxyapatite coated iron oxide nanoparticles: a promising nanomaterial for magnetic hyperthermia cancer treatment. *Nanomaterials (Basel)*, 7(12): 426 (DOI: 10.3390/nano7120426).
- [14] Chauhan, A.; Kumar, R.; Singh, P. *et al.* (2020). RF hyperthermia by encapsulated Fe<sub>3</sub>O<sub>4</sub> nanoparticles induces cancer cell death *via* time-dependent caspase-3 activation. *Nanomedicine (Lond)*, 15(4): 355-379.
- [15] Veiseh, O.; Kievit F. M.; Fang, C. *et al.* (2010). Chlorotoxin bound magnetic nanovector tailored for cancer cell targeting, imaging, and siRNA delivery. *Biomaterials*, 31(31): 8032-8042.
- [16] Bae, K. H.; Park, M.; Do, M. J. *et al.* (2012). Chitosan oligosaccharide-stabilized ferrimagnetic iron oxide nanocubes for magnetically modulated cancer hyperthermia. *ACS Nano*, 6(6): 5266-5273.
- [17] Hosseinzadeh, H.; Atyabi, F.; Dinarvand, R. *et al.* (2012). Chitosan-pluronic nanoparticles as oral delivery of anticancer gemcitabine: preparation and *in vitro* study. *Int J Nanomedicine*, 7: 1851-1863.
- [18] Kowalik, P.; Mikulski, J.; Borodziuk, A. *et al.* (2020). Yttrium-doped iron oxide nanoparticles for magnetic hyperthermia applications. *J Phys Chem C*, 124(12): 6871-6883.
- [19] Johannsen, M.; Thiesen, B.; Jordan, A. *et al.* (2005). Magnetic fluid hyperthermia (MFH) reduces prostate cancer growth in the orthotopic Dunning R3327 rat model. *Prostate*, 64(3): 283-292.
- [20] Wang, L.; Dong, J.; Ouyang, W. *et al.* (2012). Anticancer effect and feasibility study of hyperthermia treatment of pancreatic cancer using magnetic nanoparticles. *Oncol Rep*, 27(3): 719-726.

- [21] Qi, L.; Xu, Z. and Chen, M. (2007). *In vitro* and *in vivo* suppression of hepatocellular carcinoma growth by chitosan nanoparticles. *Eur J Cancer*, 43: 184-193.
- [22] Lin, M.; Huang, J.; Zhang, J. *et al.* (2013). The therapeutic effect of PEI-Mn<sub>0.5</sub>Zn<sub>0.5</sub>Fe<sub>2</sub>O<sub>4</sub> nanoparticles/pEgr1-HSV-TK/GCV associated with radiation and magnet-induced heating on hepatoma. *Nanoscale*, 5(3): 991-1000.
- [23] Cavaliere, R.; Ciocatto, E. C.; Giovanella, B. C. *et al.* (1967). Selective heat sensitivity of cancer cells. *Biochemical and clinical studies. Cancer*, 20(9): 1351-1381.
- [24] Lee, C.-T.; Mace, T. and Repasky, E. A. (2010). Hypoxia-driven immunosuppression: a new reason to use thermal therapy in the treatment of cancer? *Int J Hyperthermia*, 26(3): 232-246.
- [25] Kuppusamy, S. and Karuppaiah, J. (2013). Screening of antiproliferative effect of chitosan on tumor growth and metastasis in T24 urinary bladder cancer cell line. *Austral-Asian J Cancer*, 12: 145-149.
- [26] Zhou, J.; Wang, X.; Du, L. *et al.* (2011). Effect of hyperthermia on the apoptosis and proliferation of CaSki cells. *Mol Med Rep*, 4: 187-191.
- [27] Weyhenmeyer, B.; Murphy, A. C.; Prehn, J. H. M. *et al.* (2012). Targeting the anti-apoptotic Bcl-2 family members for the treatment of cancer. *Exp Oncol*, 34(3): 192-199.
- [28] Zavareh, H. S.; Pourmadadi, M.; Moradi, A. *et al.* (2020). Chitosan/carbon quantum dot/aptamer complex as a potential anticancer drug delivery system towards the release of 5-fluorouracil. *Int J Biol Macromol*, 165(Pt A): 1422-1430.
- [29] Jordan, A.; Scholz, R.; Wust, P. *et al.* (1997). Effects of magnetic fluid hyperthermia (MFH) on C3H mammary carcinoma *in vivo*. *Int J Hyperthermia*, 13(6): 587-605.
- [30] Salimi, M.; Sarkar, S.; Hashemi, M. *et al.* (2020). Treatment of breast cancer-bearing BALB/c mice with magnetic hyperthermia using dendrimer functionalized iron-oxide nanoparticles. *Nanomaterials (Basel)*, 10(11): 2310 (DOI: 10.3390/nano10112310).

**How to cite this article:**

Hassan, H. A.; Ebnalwaled, K.; Gedawy, H. Y. and Mahrous, N. S. (2024). The therapeutic effects of magnetic nanoparticles hyperthermia on liver cancer: *in vitro* and *in vivo* studies. *Egyptian Journal of Zoology*, 81: 76-90 (DOI: 10.21608/ejz.2023.224673.1101).

## التأثيرات العلاجية لارتفاع حرارة الجسيمات النانوية المغناطيسية على سرطان الكبد: دراسات معملية وفي الجسم الحي

حميلي عبد الشافي حسن<sup>1</sup>، خالد بن الوليد عبد الفتاح<sup>2,3</sup>، هدي يس جداوي<sup>1</sup>،  
نادية سمير محروس<sup>1</sup>

<sup>1</sup>قسم علم الحيوان، كلية العلوم، جامعة جنوب الوادي، قنا، جمهورية مصر العربية  
<sup>2</sup>مختبر الإلكترونيات والأجهزة النانوية، قسم الفيزياء، كلية العلوم، جامعة جنوب الوادي، قنا، جمهورية مصر العربية  
<sup>3</sup>كلية تكنولوجيا النانو للدراسات العليا، جامعة القاهرة، الشيخ زايد، الجيزة، جمهورية مصر العربية

ارتفاع حرارة السائل المغناطيسي هو علاج حديث للسرطان يقوم بشكل انتقائي بتسخين أنسجة الورم لتدميرها دون الإضرار بالأنسجة السليمة. تهدف الدراسة الحالية إلى تقييم التأثير السام للخلايا الناجم عن ارتفاع حرارة جسيمات مركب  $Fe_3O_4$ /الشيتوزان النانوية على سرطان الكبد في كل من المختبر والجسم الحي. تم تحضير المركب النانوي باستخدام تقنية الترسيب المشترك، وتم قياس خواصه المغناطيسية والبصرية مع طيف رامان. كما تم اختبار سمية الخلايا لجسيمات مركب  $Fe_3O_4$ /الشيتوزان النانوية على خطوط خلايا سرطان الكبد (HepG2) باستخدام قياس 3-(4,5-ثنائي ميثيل ثيازول-2-يل) 2،5-ثنائي فينيل تيترازوليوم بروميد (MTT)، وتم إجراء قابلية بقاء الخلايا بعد التعرض إلى ارتفاع حرارة جسيمات مركب  $Fe_3O_4$ /الشيتوزان النانوية باستخدام صيغة التريبان الزرقاء. بالنسبة للتجارب في الجسم الحي، تم تخصيص "25" فأراً من ذكور الفئران المهقاء (BALB/c) بشكل عشوائي ومتساوي إلى خمس مجموعات: المجموعة الأولى كانت المجموعة الضابطة غير الورمية، وشملت المجموعة الثانية الفئران الحاملة للورم، وشملت المجموعة الثالثة الفئران الحاملة للورم التي تلقت جسيمات مركب  $Fe_3O_4$ /الشيتوزان النانوية (90 مجم/كجم، مرة/أسبوع لمدة أسبوعين) عن طريق الحقن العضلي، وشملت المجموعتان الرابعة والخامسة الفئران الحاملة للورم التي تلقت جسيمات مركب  $Fe_3O_4$ /الشيتوزان النانوية عن طريق الحقن العضلي وتعرضتا لمجال مغناطيسي متناوب بتردد "200" كيلو هرتز وتيار "300 أمبير" مرة أو مرتين أسبوعياً، على التوالي، لمدة أسبوعين. أظهرت النتائج أن مركب النانو كان قادراً على إحداث سمية خلوية في المختبر، وتسبب في الموت المبرمج ونكزة الخلايا السرطانية، وتقليل حجم الورم بدرجة ملحوظة إحصائياً في الجسم الحي، عند تعرضها لمجال مغناطيسي عالي الحرارة. في الختام، يمكن أن تكون جسيمات مركب  $Fe_3O_4$ /الشيتوزان النانوية خياراً علاجياً واعداً لسرطان الكبد من خلال تقنية التسخين المغناطيسي.